Effective Theory of Nonadiabatic Quantum Evolution Based on the Quantum Geometric Tensor

O. Bleu,[1] G. Malpuech,[1] Y. Gao,[2] and D. D. Solnyshkov[1]

[1]*Institut Pascal, PHOTON-N2, University Clermont Auvergne, CNRS, 4 avenue Blaise Pascal, 63178 Aubière Cedex, France*

[2]*Department of Physics, Carnegie-Mellon University, Pittsburgh, Pennsylvania 15213, USA*

(Received 14 November 2017; published 9 July 2018)

We study the role of the quantum geometric tensor (QGT) in the evolution of two-band quantum systems. We show that all its components play an important role on the extra phase acquired by a spinor and on the trajectory of an accelerated wave packet in any realistic finite-duration experiment. While the adiabatic phase is determined by the Berry curvature (the imaginary part of the tensor), the nonadiabaticity is determined by the quantum metric (the real part of the tensor). We derive, for geodesic trajectories (corresponding to acceleration from zero initial velocity), the semiclassical equations of motion with nonadiabatic corrections. The particular case of a planar microcavity in the strong coupling regime allows us to extract the QGT components by direct light polarization measurements and to check their effects on the quantum evolution.

DOI: 10.1103/PhysRevLett.121.020401

In 1984, Berry [1] showed that the quantum evolution in a parameter space leads to the accumulation of an extra phase in the wave function, the famous Berry phase (already known in optics as the Pancharatnam phase [2]). Over the last decades, this concept and its generalization—Berry curvature—were understood to be among the most general in physics. For instance, the topological insulators [3] are classified by the Chern number [4]—an integer topological invariant obtained by integrating the Berry curvature over a complete energy band. Berry curvature also strongly affects the trajectory of an accelerated wave packet (WP), creating a lateral drift: an anomalous velocity, transverse to the acceleration. This anomalous velocity is at the origin of many crucial phenomena in physics such as the anomalous Hall effect (AHE) [5–7] including transverse conductivity in Weyl metals [8–10], the intrinsic spin Hall effect for electrons [11] and light [12,13], or the valley Hall effect [14–16] in transition metal dichalcogenides (TMDs), the latter being a pillar of the emerging field called "valleytronics" [17].

However, Berry curvature is a part of a more general object: the quantum geometric tensor (QGT). The gauge-invariant QGT was introduced in 1980 by Provost and Vallee [18] as a part of a geometric approach to quantum mechanics [19]. Its imaginary part corresponds to the Berry curvature [1,20], whereas its real part defines a Riemannian metric, which allows us to measure the distance between quantum states, involved in the definition of fidelity, main figure of merit in quantum computing [21,22] (including photonics [23]). Quantum metric also appears in the recent studies of phase transitions [24–26]. In condensed matter, the real part of the QGT has been linked to the superfluid fraction of flat bands [27,28], to current noise in an insulator [26], to Lamb shift analog for exciton states in TMDs [29], and to orbital magnetic susceptibility in Bloch bands [30,31].

The two parts of the QGT play complementary roles when the Hamiltonian of the system changes over time. The imaginary part (Berry curvature) defines the additional Berry phase in the adiabatic limit, while the real part (quantum distance) determines the nonadiabaticity (NA), which, in turn, brings a correction to the Berry's formalism. NA in quantum systems has been studied extensively since the pioneering works of Landau [32,33], Zener [34], Dykhne [35], and many others [36–39], concerning the regime where the NA is exponentially small, whereas configurations with power-law NA were generally considered as somewhat less interesting [35,40]. The Landau quasiclassical formalism allows us to calculate the final nonadiabatic fraction (transition probability) when the perturbation smoothly vanishes at infinities. However, this approach cannot be applied to a simple yet important situation of a magnetic field rotating with a constant angular velocity, because the perturbation does not vanish. Berry himself trusted that the NA is exponentially small [1], but that is not the case in the configuration he considered [41,42], as we shall see below. Moreover, the NA changes during the evolution, and its final value is different from the maximal one. The Landau-Zener formalism allows us to find only the former, while the latter is not exponentially small even if the evolution is perfectly smooth. In all these cases, the real part of the QGT allows us to quantify the NA and brings an important correction to the Berry phase.

In this work, we calculate the nonadiabatic corrections (NAC) for the phases and trajectories of WPs for a finite-time quantum evolution beyond the Landau-Zener approximation, considering the important family of geodesic trajectories, corresponding to acceleration from zero initial velocity. We show that these NACs are quantitatively described by the real part of the QGT, whereas the adiabatic limit is described by the imaginary part (Berry phase). We propose a specific example of application: a planar microcavity [43] in the strong coupling regime. We show that it allows, through simple light polarization measurements, a direct access to the components of the QGT, providing an answer to an important problem of recent years—the direct measurement of Berry curvature and geometric quantities [44–52]. We consider a practical experimental situation showing how the real and imaginary part of the QGT control the AHE.

Rotation of a spin.—The Bloch sphere represents the simplest 2-level system with Berry curvature: a spin, interacting with an applied magnetic field. Any 2-level Hamiltonian can be written as a superposition of Pauli matrices, and thus considered as an effective field acting on a pseudospin.

A spin, which follows a slowly rotating magnetic field, is never perfectly aligned with it, and thus it exhibits fast precession (frequency Ω) about the magnetic field together with the slow rotation (ω) of both of them in the azimuthal plane [Fig. 1(a)]. This behavior is similar to the rotation of a small wheel attached to a long shaft [Fig. 1(b)]: the wheel, rotating around its axis with the angular frequency Ω, at the same time rotates with the frequency ω around the shaft fixation point. For both the spin and the wheel, there is an important rotational energy associated with the large frequency Ω, but another part of the energy is associated with the circular motion ω. Nobody could think of neglecting the kinetic energy of the wheel's motion $mv^2/2$. However, the energy of the spin's slow rotation encoded in the Berry phase has been less evident to see. It can be obtained by applying the energy operator $\hat{E} = i\hbar\partial/\partial t$ to the rotating spinor $\psi(t) = 1/\sqrt{2}(e^{-i\omega t}, 1)^T e^{i\Omega t/2}$ (valid in the limit $\omega \to 0$), which gives $\langle \hat{E} \rangle = -\hbar\Omega/2 + \hbar\omega/2$. The first term in this expression is the usual energy of the spin in the magnetic field ("dynamical phase"), and the second is the energy associated with the Berry phase which appears because of the time dependence of the spinor. For the time $T = 2\pi/\omega$ of one full rotation of the field it gives $\gamma_B = \hbar\omega T/\hbar = \pi$. One can then take a derivative over the parameters of the wave function (WF), to get rid of the explicit time dependence $i\langle\psi|\partial\psi/\partial t\rangle = i\langle\psi|\partial\psi/\partial\varphi\rangle\partial\varphi/\partial t$.

Because of the finite experiment duration, the spin does not perfectly follow the field and gets out of the azimuthal plane, tracing a cycloidal trajectory. The corresponding WF reads

$$\psi(t) = \begin{pmatrix} \cos\frac{\theta(t)}{2} e^{-i\omega t} \\ \sin\frac{\theta(t)}{2} \end{pmatrix} e^{i[\Omega\cos\xi(t)/2]t}, \qquad (1)$$

where θ is the polar angle and ξ is the angle between the field and the spin. Averaging this expression over precession time allows obtaining the correction to the energy. The average value of θ for the cycloidal trajectory of Fig. 1(a) corresponds to the equilibrium (zero precession [42,53,54]) polar angle $\theta = \pi/2 - \omega/\Omega$, giving [53] $E = -\hbar\Omega/2 + \hbar\omega/2(1 + 2\omega/\Omega)$, and a final extra phase $\gamma = \pi(1 + 2\omega/\Omega)$ or $\Delta\gamma/\gamma_B = 4\pi/(\Omega T)$ for one full rotation time T.

The total extra phase after one full rotation of the magnetic field from the numerical solution of the Schrödinger equation is plotted in Fig. 1(c) as a function of the rotation duration T measured in units of precession periods $2\pi/\Omega$ (equivalent to the frequency ratio Ω/ω). Larger T means slower rotation and the adiabatic limit corresponds to $T \to \infty$ or $\omega/\Omega \to 0$. We see that the extra phase indeed converges to the value π, but the correction is not negligible: $\Delta\gamma/\gamma_B > 30\%$ for $\omega > \Omega/10$. The difference between the exact extra phase and the adiabatical value of π is shown in a log-log plot on Fig. 1(d), again as a function of T (black curve). We see that instead of being exponentially small, this correction decreases only as $1/T$. The analytical NAC, $\Delta\gamma/\gamma_B = 4\pi/(\Omega T)$ (red curve), fits the exact result very well [53].

Quantum geometric tensor.—The QGT allows us to generalize the above development to an arbitrary parameter space and to unite both contributions to the extra phase acquired by the WF in a single mathematical entity. In general, a metric tensor g_{ij} determines how the distance ds between two infinitesimally separated points depends on the difference of their coordinates λ_i:

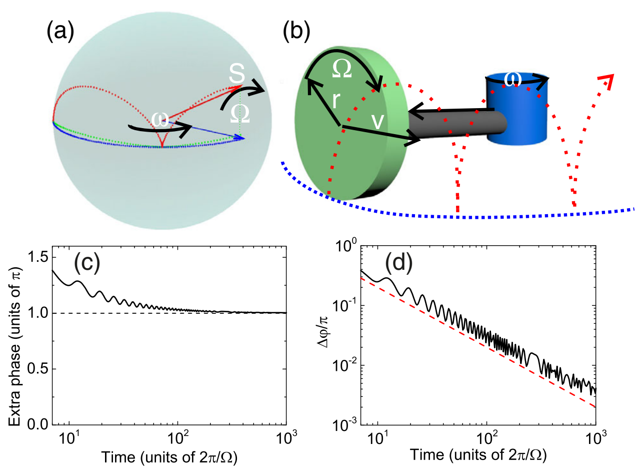

FIG. 1. (a) Bloch sphere with the spin (red arrow) and the magnetic field Ω (blue arrow), adiabatic trajectory (blue), and real trajectory (red dashed line). (b) Mechanical analog: adiabatic trajectory of an infinitely small wheel (blue), cycloid trajectory of a point on a wheel (red). Ω—wheel rotation frequency, v—wheel velocity, ω—shaft center rotation. (c) Total extra phase for one full spinor rotation as a function of the rotation time. (d) Deviation from the adiabatic Berry phase: numerical calculation (black) and analytical correction exhibiting $1/T$ decay (red dashed).

$$ds^2 = g_{ij} d\lambda_i d\lambda_j. \tag{2}$$

In the space of quantum-mechanical eigenstates, the distance is measured by the Fubini-Study metric, determined by the WF overlap $ds^2 = 1 - |\langle\psi(\lambda)|\psi(\lambda+\delta\lambda)\rangle|^2$. Minimal distance $ds = 0$ corresponds to a maximal overlap of 1, while maximal distance $ds = 1$ corresponds to orthogonal states. At each point of the Hilbert space, the metric is thus determined by the WF $\psi(\lambda)$, and the corresponding metric tensor is defined [18] as the real part of the QGT:

$$T_{ij} = \left\langle \frac{\partial}{\partial\lambda_i}\psi \middle| \frac{\partial}{\partial\lambda_j}\psi \right\rangle - \left\langle \frac{\partial}{\partial\lambda_i}\psi \middle| \psi \right\rangle \left\langle \psi \middle| \frac{\partial}{\partial\lambda_j}\psi \right\rangle, \tag{3}$$

where ψ is the WF, λ_i and λ_j are the coordinates in the parameter space (see Ref. [53] for details). Later, it was understood that the imaginary part of QGT is the Berry curvature [20],

$$|\mathbf{B}| = 2\Im[T_{ij}] = \Im[\nabla_\lambda \times \langle\psi(\lambda)|\nabla_\lambda\psi(\lambda)\rangle], \tag{4}$$

which determines the Berry phase for a closed path in the parameter space.

Both components of the QGT contribute to the phase of the WF in any finite-duration experiment: Berry curvature determines the adiabatic value, while the quantum metric allows us to determine a NAC. The average NA fraction (fraction of the excited state in the WF) for a spin on the Bloch sphere can be found as $f_{\mathrm{NA,eq}} = \omega^2/4\Omega^2$ [53], which is generalized using $\omega(\lambda) = 2ds/dt = 2\sqrt{g_{\lambda\lambda}(\lambda)}d\lambda/dt$ and $\Omega = \Omega(\lambda)$:

$$f_{\mathrm{NA,eq}}(\lambda) = \frac{g_{\lambda\lambda}}{\Omega^2}\left(\frac{d\lambda}{dt}\right)^2. \tag{5}$$

QGT and WP trajectory.—Berry curvature has been shown to affect the trajectory of accelerated WPs, creating an anomalous velocity contribution in the AHE [5,6]. The semiclassical equations of motion for the center of mass of a quantum WP in the presence of Berry curvature can be derived using the Lagrangian formalism [6,55–58]):

$$\hbar\frac{\partial\mathbf{k}}{\partial t} = \mathbf{F}, \qquad \hbar\frac{\partial\mathbf{r}}{\partial t} = \frac{\partial\epsilon}{\partial\mathbf{k}} - \hbar\frac{\partial\mathbf{k}}{\partial t}\times\mathbf{B}, \tag{6}$$

where ϵ is the energy dispersion, $\mathbf{B}(k)$ is the Berry curvature, and $\mathbf{F}$ is an external conservative force, accelerating the WP. For charged particles, $\mathbf{F} = q\mathbf{E}$. Magnetic forces, known to affect the magnetic susceptibility [30,31,59], are not the subject of the present work. Different types of corrections to these equations have been considered in the past [60–62]. NACs account for the fact that the WF is a superposition of two eigenstates $\psi = f_0\psi_0 + f_1\psi_1$ (where $|f_1|^2 = f_{NA}$ found above). Their respective energies contribute both to the first term: $\tilde{\epsilon}(k) = |f_0|^2\epsilon_0(k) + |f_1|^2\epsilon_1(k)$, ultimately providing a second-order correction to the group velocity. Other NACs concern the second term, and, in a general case, the first-order corrections should dominate.

Along geodesic lines (the most important case corresponding to acceleration from $v = 0$ under a constant force $\mathbf{F}$, as in the Hall effect), all first-order and second-order corrections cancel, except one. This single correction appears because the metric along the true trajectory of ψ is not the same as the one along the equator of the Bloch sphere (followed by the eigenstates ψ_0 and ψ_1). Indeed,

$$\left\langle\psi\middle|\frac{d}{dt}\psi\right\rangle = \left\langle\psi\middle|\frac{d}{ds_s}\psi\right\rangle\frac{ds_s}{dt} = \left\langle\psi\middle|\frac{d}{d\varphi}\psi\right\rangle\frac{d\varphi}{ds_s}\frac{ds_s}{dt}, \tag{7}$$

where $d\varphi/ds_s = 1/\sqrt{g_{\varphi\varphi}} = 1/r\sin\theta$. Now, we can write ψ and the Berry connection on the basis of the eigenstates (which are on the equator, where $ds_s = d\varphi$),

$$\frac{1}{\sin\theta}\left\langle f_i\psi_i\middle|\frac{d}{d\varphi}f_i\psi_i\right\rangle\frac{ds_s}{dt} = \frac{1}{\sin\theta}\left\langle f_i\psi_i\middle|\frac{d}{dt}f_i\psi_i\right\rangle. \tag{8}$$

The Berry connection above involves intra- and interband terms [61]. For the Berry curvature appearing in the AHE, the intraband terms add up to 1, while the interband terms cancel out, giving simply $B = B_0/\sin\theta$, where B_0 is the Berry curvature of the instantaneous eigenstate ψ_0. The Lagrangian formalism provides [53] the corrected equation for the trajectory

$$\hbar\frac{\partial\mathbf{r}}{\partial t} = \frac{\partial\tilde{\epsilon}}{\partial\mathbf{k}} + \hbar\frac{\partial\mathbf{k}}{\partial t}\times 2\Im[\mathbf{T}_{k\phi}]\left(1 + 2\frac{T_{kk}}{\Omega^2}\left(\frac{\partial\mathbf{k}}{\partial t}\right)^2\right) \tag{9}$$

This equation is the main result of our Letter. It shows that the anomalous velocity is a sum of the adiabatic value [as in Eq. (6)] and a NAC (the second term in the parenthesis). We stress that this equation is only valid when the field follows a geodesic trajectory in the parameter space. In such case, while the renormalized energy $\tilde{\epsilon}$ brings second-order corrections to the acceleration in the direction of the force, the anomalous velocity only includes the correction from the variation of the metric due to the NA, because the other first- and second-order corrections to this term cancel out. Since the transverse conductivity arising from the anomalous velocity is known to be determined by the integral of the Berry curvature (e.g., in Weyl metals [8–10]), its NAC could be linked with the integral of the quantum metric (the Euler characteristic). The NAC is similar to the relativistic correction in the Kepler problem: like the curvature of the radial Schwarzschild metric perturbs its interplay with the azimuthal part, leading to the perihelion precession, Berry curvature also inevitably brings quantum metric curvature, affecting the trajectory.

QGT in a planar cavity.—Exploring the whole Bloch sphere requires all 3 components of the effective magnetic

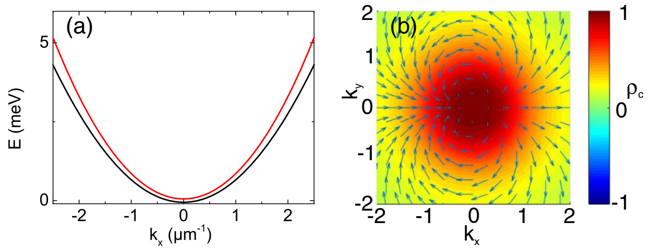

FIG. 2. (a) LPB split by Zeeman field and TE-TM SOC. (b) Pseudospin texture of the lower eigenstate: In-plane pseudospin projection (arrows) and S_Z (color).

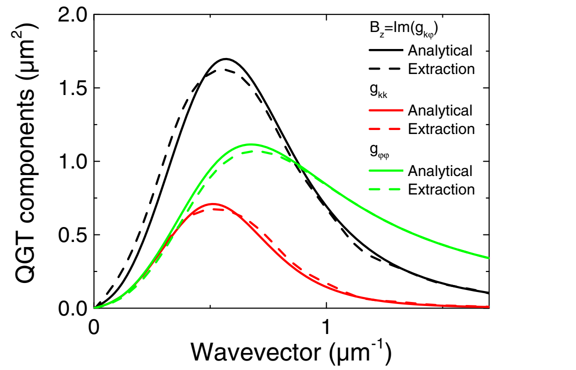

FIG. 3. QGT components: B_Z (black), g_{kk} (red), and $g_{\phi\phi}$ (green) calculated analytically (solid lines) and extracted from numerical experiment (dashed lines).

field. If one deals with light, it means controlling the splittings between linear and circular polarizations. This is why we have chosen a model system consisting of a microcavity in the strong coupling regime [43], where the polariton modes appear from exciton and photon resonances. The photonic fraction provides a βk^2 in-plane spin-orbit coupling (SOC) due to the TE-TM splitting [63,64], while the exciton mode provides the Zeeman splitting Δ [65,66] (under applied magnetic field or thanks to spin-anisotropic interactions [67]). Here, the pseudospin can be easily measured via the polarization of light [53].

We begin with the parabolic spinor Hamiltonian of the lower polariton branch (LPB) of a planar cavity:

$$H_0 = \begin{pmatrix} \frac{\hbar^2 k^2}{2m^*} + \Delta & \beta k^2 e^{2i\phi} \\ \beta k^2 e^{-2i\phi} & \frac{\hbar^2 k^2}{2m^*} - \Delta \end{pmatrix}, \tag{10}$$

with the following eigenvalues [Fig. 2(a)]:

$$\epsilon_{\pm}(k) = \frac{\hbar^2 k^2}{2m^*} \pm \sqrt{(\Delta^2 + \beta^2 k^4)}, \tag{11}$$

with $\Delta = 60\ \mu\text{eV}$, $\beta = 0.14\ \text{meV}/\mu\text{m}^{-2}$. While the system shows no gap because of the positive mass of both branches, and therefore is not a topological insulator, it nevertheless exhibits a nonzero Berry curvature, reflected by the pseudospin texture [Fig. 2(b)], similar to bilayer graphene under bias voltage [68–70]. We compute analytically the QGT for the lower eigenstate in polar coordinates (k,ϕ):

$$g_{kk} = \frac{\Delta^2 k^2 \beta^2}{(\Delta^2 + \beta^2 k^4)^2}, \qquad g_{\phi\phi} = \frac{k^2 \beta^2}{\Delta^2 + \beta^2 k^4},$$
$$g_{k\phi} = g_{\phi k} = 0, \qquad \mathbf{B} = \frac{2\Delta k^2 \beta^2}{(\Delta^2 + k^4 \beta^2)^{3/2}} \mathbf{e_Z}. \tag{12}$$

These are plotted as solid curves in Fig. 3. Because of the k^2 dependence of the TE-TM SOC, the form of the Berry curvature is different from the one of Rashba SOC [7,57] (with maximum at $k = 0$) and similar to the one of bilayer graphene [71].

A very interesting opportunity to measure the QGT directly is offered by the radiative states of photonic systems which allow us to access all pseudospin components $\mathbf{S}$ via polarization:

$$g_{kk} = \frac{1}{4} \frac{(\frac{\partial}{\partial k} S_z(k))^2}{1 - S_z(k)^2}, \tag{13}$$

$$g_{\phi\phi} = \frac{1}{4k^2} \left(\frac{\frac{\partial}{\partial \phi} (\frac{S_y}{S_x})}{1 + (\frac{S_y}{S_x})^2} \right)^2 (1 - S_z^2), \tag{14}$$

$$|\mathbf{B}| = \frac{1}{2k} \left(\frac{\frac{\partial}{\partial \phi} (\frac{S_y}{S_x})}{1 + (\frac{S_y}{S_x})^2} \right)^2 \frac{\partial S_z}{\partial k}. \tag{15}$$

To demonstrate that the QGT components including the Berry curvature can indeed be extracted from a realistic experiment, we perform a numerical simulation using a 2D spinor Schrödinger equation for LPB in the parabolic approximation,

$$i\hbar \frac{\partial \psi_\pm}{\partial t} = -\frac{\hbar^2}{2m} \Delta \psi_\pm - \frac{i\hbar}{2\tau} \psi_\pm + \Delta \psi_\pm + \beta \left(\frac{\partial}{\partial x} \mp i \frac{\partial}{\partial y} \right)^2 \psi_\mp + \hat{P}, \tag{16}$$

where $\psi_+(\mathbf{r}, t), \psi_-(\mathbf{r}, t)$ are the two circular components, $m = 5 \times 10^{-5} m_{\text{el}}$ is the polariton mass, $\tau = 30$ ps the lifetime, and $\hat{P}$ is the pump operator, which in this case represents uncorrelated noise describing the spontaneous scattering under nonresonant pumping of the exciton reservoir. The results of the extraction are presented in Fig. 3 as dashed curves, whose perfect agreement with the solid lines obtained from Eq. (12) confirms the validity of this method.

Figure 4(a) shows the trajectories of polariton WP accelerated in a microcavity by a realistic wedge $U(x) = -Fx$, where $F = 1\ \text{meV}/128\ \mu\text{m}$ for 4 values of β. The red-dashed

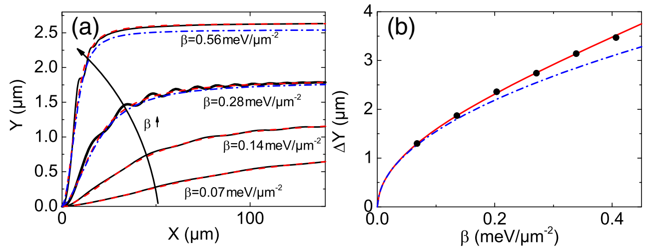

FIG. 4. (a) WP trajectories in real space: Numerical (black) and analytical (red dashed, uncorrected–blue dash-dotted) for 3 values of TE-TM SOC β ($\Delta = 0.06$ meV). (b) Final lateral shift as a function of β: adiabatic (blue dash-dotted line), corrected (red solid line), and numerical (black dots). Here, $\Delta = 0.03$ meV.

curves calculated using equation (9) (accounting for both $\Re[T]$ and $\Im[T]$) are in excellent agreement with direct numerical solution of the Schrödinger equation (16) (black curves). The NA fraction can be extracted experimentally from polarization [53]: $f_{\mathrm{NA}} = S_Y^2$. The blue dotted curve shows the trajectory without the correction (based only on $\Im[T]$). The difference becomes more important for higher gradients. Figure 4(b) shows the final lateral shift ΔY as a function of β: adiabatic [$\Delta Y = \sqrt{\beta}\Gamma^2(3/4)/\sqrt{\Delta\pi}$—blue dotted [53]] and corrected (red) curves, as well as results of simulations (black dots). Numerical results are much better fitted by the theory including the NAC. Both the *relative* lateral shift and the NAC are comparable to the values reported for metamaterials [72]. Such effects could be important for applications in integrated polaritonics.

To conclude, we derive a new correction to the semiclassical equations of motion of an accelerated WP on geodesic trajectories in two-band systems appearing in any realistic finite-duration experiment. While the adiabatic limit is determined by the Berry curvature, the NAC is determined by the quantum metric. This correction brings a nonlinear contribution to the transverse conductivity. The particular case of a planar microcavity in strong coupling regime allows us to extract the QGT components by direct measurements and to check their effects on the quantum evolution.

We thank F. Piechon and J. N. Fuchs for useful discussions. We acknowledge the support of the project "Quantum Fluids of Light" (ANR-16-CE30-0021), of the ANR Labex Ganex (ANR-11-LABX-0014), and of the ANR program "Investissements d'Avenir" through the IDEX-ISITE initiative 16-IDEX-0001 (CAP 20-25). Y. G. is supported by the Department of Energy, Basic Energy Sciences, Materials Sciences and Engineering Division, Grant No. DE-SC0012509. D. D. S. acknowledges the support of IUF (Institut Universitaire de France).

Note added in proofs.—Recently, we became aware of a work by A. Gutierrez-Rubio *et al.* [73], devoted to polariton anomalous Hall effect, which we consider as an illustration in the second part.

[1] M. V. Berry, Proc. R. Soc. **392**, 45 (1984).
[2] S. Pancharatnam, Proc. Indian Acad. Sci. A **44**, 127 (1956).
[3] M. Z. Hasan and C. L. Kane, Rev. Mod. Phys. **82**, 3045 (2010).
[4] S. S. Chern, Ann. Math. Second Series **47**, 85 (1946).
[5] R. Karplus and J. M. Luttinger, Phys. Rev. **95**, 1154 (1954).
[6] G. Sundaram and Q. Niu, Phys. Rev. B **59**, 14915 (1999).
[7] N. Nagaosa, J. Sinova, S. Onoda, A. H. MacDonald, and N. P. Ong, Rev. Mod. Phys. **82**, 1539 (2010).
[8] A. A. Burkov and L. Balents, Phys. Rev. Lett. **107**, 127205 (2011).
[9] A. A. Burkov, Phys. Rev. Lett. **113**, 187202 (2014).
[10] J. F. Steiner, A. V. Andreev, and D. A. Pesin, Phys. Rev. Lett. **119**, 036601 (2017).
[11] J. Sinova, D. Culcer, Q. Niu, N. A. Sinitsyn, T. Jungwirth, and A. H. MacDonald, Phys. Rev. Lett. **92**, 126603 (2004).
[12] K. Y. Bliokh, A. Niv, V. Kleiner, and E. Hasman, Nat. Photonics **2**, 748 (2008).
[13] X. Ling, X. Zhou, K. Huang, Y. Liu, C.-W. Qiu, H. Luo, and S. Wen, Rep. Prog. Phys. **80**, 066401 (2017).
[14] D. Xiao, W. Yao, and Q. Niu, Phys. Rev. Lett. **99**, 236809 (2007).
[15] K. F. Mak, K. L. McGill, J. Park, and P. L. McEuen, Science **344**, 1489 (2014).
[16] X. Xu, W. Yao, D. Xiao, and T. F. Heinz, Nat. Phys. **10**, 343 (2014).
[17] J. R. Schaibley, H. Yu, G. Clark, P. Rivera, J. S. Ross, K. L. Seyler, W. Yao, and X. Xu, Nat. Rev. Mater. **1**, 16055 (2016).
[18] J. Provost and G. Vallee, Commun. Math. Phys. **76**, 289 (1980).
[19] J. Anandan and Y. Aharonov, Phys. Rev. Lett. **65**, 1697 (1990).
[20] M. Berry, in *Geometric Phases in Physics* (World Scientific, Singapore, 1989), p. 7.
[21] K. Życzkowski and H.-J. Sommers, Phys. Rev. A **71**, 032313 (2005).
[22] D. Leibfried, B. DeMarco, V. Meyer, D. Lucas, M. Barrett, J. Britton, W. M. Itano, B. Jelenkovic, C. Langer, T. Rosenband *et al.*, Nature (London) **422**, 412 (2003).
[23] P. Kok, W. J. Munro, K. Nemoto, T. C. Ralph, J. P. Dowling, and G. J. Milburn, Rev. Mod. Phys. **79**, 135 (2007).
[24] P. Zanardi, P. Giorda, and M. Cozzini, Phys. Rev. Lett. **99**, 100603 (2007).
[25] M. Kolodrubetz, V. Gritsev, and A. Polkovnikov, Phys. Rev. B **88**, 064304 (2013).
[26] T. Neupert, C. Chamon, and C. Mudry, Phys. Rev. B **87**, 245103 (2013).
[27] S. Peotta and P. Törmä, Nat. Commun. **6**, 8944 (2015).
[28] A. Julku, S. Peotta, T. I. Vanhala, D.-H. Kim, and P. Törmä, Phys. Rev. Lett. **117**, 045303 (2016).
[29] A. Srivastava and A. Imamoglu, Phys. Rev. Lett. **115**, 166802 (2015).
[30] Y. Gao, S. A. Yang, and Q. Niu, Phys. Rev. B **91**, 214405 (2015).
[31] F. Piéchon, A. Raoux, J.-N. Fuchs, and G. Montambaux, Phys. Rev. B **94**, 134423 (2016).
[32] L. D. Landau, Phys. Z. Sowjetunion **1**, 88 (1932).
[33] L. D. Landau, Phys. Z. Sowjetunion **2**, 46 (1932).
[34] C. Zener, Proc. R. Soc. A **137**, 696 (1932).

[35] A. M. Dykhne, ZhETF **38**, 570 (1960) [Sov. Phys. JETP **11**, 411 (1960)].
[36] L. D. Landau and E. Teller, Phys. Z. Sowjetunion **10**, 34 (1936).
[37] E. C. G. Stueckelberg, Helv. Phys. Acta **5**, 369 (1932).
[38] J. P. Davis and P. Pechukas, J. Chem. Phys. **64**, 3129 (1976).
[39] S. Shevchenko, S. Ashhab, and F. Nori, Phys. Rep. **492**, 1 (2010).
[40] L. D. Landau and E. M. Lifshitz, *Quantum Mechanics: Non-Relativistic Theory* (Pergamon Press, New York, 1991).
[41] K. Y. Bliokh, Phys. Lett. A **372**, 204 (2008).
[42] S. Oh, X. Hu, F. Nori, and S. Kais, Sci. Rep. **6**, 20824 (2016).
[43] A. Kavokin, J. J. Baumberg, G. Malpuech, and F. P. Laussy, *Microcavities* (Oxford University Press, New York, 2011).
[44] M. Onoda, S. Murakami, and N. Nagaosa, Phys. Rev. Lett. **93**, 083901 (2004).
[45] G. Jotzu, M. Messer, R. Desbuquois, M. Lebrat, T. Uehlinger, D. Greif, and T. Esslinger, Nature (London) **515**, 237 (2014).
[46] T. Ozawa and I. Carusotto, Phys. Rev. Lett. **112**, 133902 (2014).
[47] M. Hafezi, Phys. Rev. Lett. **112**, 210405 (2014).
[48] H. M. Price, O. Zilberberg, T. Ozawa, I. Carusotto, and N. Goldman, Phys. Rev. B **93**, 245113 (2016).
[49] N. Flaschner, B. S. Rem, M. Tarnowski, D. Vogel, D.-S. Luhmann, K. Sengstock, and C. Weitenberg, Science **352**, 1091 (2016).
[50] M. Wimmer, H. M. Price, I. Carusotto, and U. Peschel, Nat. Phys. **13**, 545 (2017).
[51] L.-K. Lim, J.-N. Fuchs, and G. Montambaux, Phys. Rev. A **92**, 063627 (2015).
[52] L.-K. Lim, J.-N. Fuchs, and G. Montambaux, Phys. Rev. A **91**, 042119 (2015).
[53] See Supplemental Material at http://link.aps.org/supplemental/10.1103/PhysRevLett.121.020401 for details on the quantum geometric tensor, spin dynamics, and semi-classical equations with non-adiabatic corrections.
[54] H.-A. Engel, E. I. Rashba, and B. I. Halperin, *Theory of Spin Hall Effects in Semiconductors* (John Wiley and Sons, Ltd., New York, 2007), ISBN: 9780470022184.
[55] M.-C. Chang and Q. Niu, Phys. Rev. Lett. **75**, 1348 (1995).
[56] D. Culcer, Y. Yao, and Q. Niu, Phys. Rev. B **72**, 085110 (2005).
[57] D. Xiao, M.-C. Chang, and Q. Niu, Rev. Mod. Phys. **82**, 1959 (2010).
[58] M.-C. Chang and Q. Niu, J. Phys. Condens. Matter **20**, 193202 (2008).
[59] D. Ceresoli, T. Thonhauser, D. Vanderbilt, and R. Resta, Phys. Rev. B **74**, 024408 (2006).
[60] P. Gosselin and H. Mohrbach, J. Phys. A **43**, 354025 (2010).
[61] Y. Gao, S. A. Yang, and Q. Niu, Phys. Rev. Lett. **112**, 166601 (2014).
[62] Y. Gao, S. A. Yang, and Q. Niu, Phys. Rev. B **95**, 165135 (2017).
[63] G. Panzarini, L. Andreani, A. Armitage, D. Baxter, M. S. Skolnick, V. N. Astratov, J. S. Roberts, A. V. Kavokin, M. R. Vladimirova, and M. A. Kaliteevski, Phys. Rev. B **59**, 5082 (1999).
[64] A. Kavokin, G. Malpuech, and M. Glazov, Phys. Rev. Lett. **95**, 136601 (2005).
[65] J. Tignon, P. Voisin, C. Delalande, M. Voos, R. Houdré, U. Oesterle, and R. P. Stanley, Phys. Rev. Lett. **74**, 3967 (1995).
[66] B. Pietka, D. Zygmunt, M. Król, M. R. Molas, A. A. L. Nicolet, F. Morier-Genoud, J. Szczytko, J. Łusakowski, P. Zieba, I. Tralle *et al.*, Phys. Rev. B **91**, 075309 (2015).
[67] M. Vladimirova, S. Cronenberger, D. Scalbert, K. V. Kavokin, A. Miard, A. Lemaître, J. Bloch, D. Solnyshkov, G. Malpuech, and A. V. Kavokin, Phys. Rev. B **82**, 075301 (2010).
[68] A. H. MacDonald, J. Jung, and F. Zhang, Phys. Scr. **T146**, 014012 (2012).
[69] E. McCann, Phys. Rev. B **74**, 161403 (2006).
[70] E. V. Castro, K. S. Novoselov, S. V. Morozov, N. M. R. Peres, J. M. B. Lopes dos Santos, J. Nilsson, F. Guinea, A. K. Geim, and A. H. Castro Neto, Phys. Rev. Lett. **99**, 216802 (2007).
[71] F. Zhang, J. Jung, G. A. Fiete, Q. Niu, and A. H. MacDonald, Phys. Rev. Lett. **106**, 156801 (2011).
[72] X. Ling, X. Zhou, X. Yi, W. Shu, Y. Liu, C. Shizhen, H. Luo, S. Wen, and D. Fan, Light: Science Appl. **4**, e290 (2015).
[73] A. Gutierrez-Rubio *et al.*, arXiv:1802.02527.